Title

Mechanisms of MAFG Dysregulation in Cholestatic Liver Injury and Development of Liver Cancer.

Journal

Gastroenterology, 155(2)

ISSN

0016-5085

Authors

Liu, Ting
Yang, Heping
Fan, Wei
et al.

Publication Date

2018-08-01

DOI

10.1053/j.gastro.2018.04.032

Peer reviewed

Accepted Manuscript

Mechanisms of MAFG Dysregulation in Cholestatic Liver Injury and Development of Liver Cancer

Ting Liu, Heping Yang, Wei Fan, Jian Tu, Tony W.H. Li, Jiaohong Wang, Hong Shen, JinWon Yang, Ting Xiong, Justin Steggerda, Zhenqiu Liu, Mazen Noureddin, Stephanie S. Maldonado, Alagappan Annamalai, Ekihiro Seki, José M. Mato, Shelly C. Lu

PII: S0016-5085(18)34482-2
DOI: 10.1053/j.gastro.2018.04.032
Reference: YGAST 61860

To appear in: *Gastroenterology*
Accepted Date: 30 April 2018

Please cite this article as: Liu T, Yang H, Fan W, Tu J, Li TWH, Wang J, Shen H, Yang J, Xiong T, Steggerda J, Liu Z, Noureddin M, Maldonado SS, Annamalai A, Seki E, Mato JM, Lu SC, Mechanisms of MAFG Dysregulation in Cholestatic Liver Injury and Development of Liver Cancer, *Gastroenterology* (2018), doi: 10.1053/j.gastro.2018.04.032.

Mechanisms of MAFG Dysregulation in Cholestatic Liver Injury and Development of Liver Cancer

Short Title: *MAFG is an oncogene in human liver cancers*

Ting Liu[1-3†], Heping Yang[1†], Wei Fan[1,4,5†], Jian Tu[1,6], Tony W. H. Li[1], Jiaohong Wang[1], Hong Shen[7], JinWon Yang[1], Ting Xiong[1, 6], Justin Steggerda[8], Zhenqiu Liu[9], Mazen Noureddin[1,10], Stephanie S. Maldonado[11], Alagappan Annamalai[8,10], Ekihiro Seki[1], José M. Mato[12], and Shelly C. Lu[1*]

[1]Division of Digestive and Liver Diseases, Cedars-Sinai Medical Center, LA, CA 90048, USA; [2]Department of Gastroenterology, Xiangya Hospital, Central South University, Changsha, Hunan 410008, China; [3]Key Laboratory of Cancer proteomics of Chinese Ministry of Health, Xiangya Hospital, Central South University, Changsha, Hunan 410008, China; [4]Department of Geriatrics, Guangzhou First People's Hospital, Guangzhou 510180, China; [5]State Key Laboratory of Respiratory Diseases, The First Affiliated Hospital, Guangzhou Medical University, Guangzhou, 510120, China; [6]Institute of Pharmacy & Pharmacology, University of South China, Hengyang 421001, China; [7]Department of Oncology, Xiangya Hospital, Central South University, Changsha, Hunan 410008, China; [8]Department of Surgery, Cedars-Sinai Medical Center; [9]Samuel Oschin Comprehensive Cancer Institute, Cedars-Sinai Medical Ceter, LA, CA 90048; [10]Comprehensive Transplant Center, Cedars-Sinai Medical Center, LA, CA 90048, USA; [11]The Warren Alpert Medical School of Brown University; [12]CIC bioGUNE, Centro de Investigación Biomédica en Red de Enfermedades Hepáticas y Digestivas (Ciberehd), Technology, Park of Bizkaia, 48160 Derio, Bizkaia, Spain

† These authors share first authorship

Financial Support: This work was supported by NIH grants R01DK092407 (HP Yang and SC Lu) and R01CA172086 (SC Lu, HP Yang, JM Mato), Agencia Estatal de Investigación MINECO SAF 2014-52097R, CIBERehd-ISCiii and Severo Ochoa Excellence Accreditation SEV-2016-0644 (to JM Mato). Changsha science and technology bureau 1701090 (to Ting Liu). The funders had no role in study design, data collection and analysis, decision to publish, or preparation of the manuscript.

List of abbreviations (in alphabetical order).
AFP, alpha-fetoprotein; AP-1, activator protein-1; ARE, antioxidant response element; BDL, bile duct ligation; BrdU, 5-Bromo-2'deoxyuridine; CCA, cholangiocarcinoma; ChIP, chromatin immunoprecipitation; CRISPR/Cas9, Clustered Regularly Interspaced Short Palindromic Repeats/CRISPR-associated protein 9; DEN, diethylnitrosamine; EMSA, electrophoretic mobility shift assay; EV, empty vector; FXR, farnesoid X receptor; GSH, reduced glutathione; HCC, hepatocellular carcinoma; H&E, hematoxylin and eosin; IHC, immunohistochemistry; KO, knockout; LCA, lithocholic acid; MAFG, V-Maf Avian Musculoaponeurotic Fibrosarcoma Oncogene Homolog G; MAT, methionine adenosyltransferase; NF-κB, nuclear factor κB; NRF2, nuclear factor-erythroid 2 related factor 2; OCA, obeticholic acid; PHB1, prohibitin 1; PBC, primary biliary cholangitis;

ROC, receiver operating characteristic; SAMe, S-adenosylmethionine; SC, scrambled; Seq-ChIP, sequential ChIP; UDCA, ursodeoxycholic acid; WT, wild type

***Corresponding author:** Shelly C. Lu, M.D., Cedars-Sinai Medical Center, Davis Building, Room #2097, 8700 Beverly Blvd., Los Angeles, CA, 90048. Tel: (310) 423-5692, Fax: (310) 423-0653, e-mail: shelly.lu@cshs.org

Conflict of interest:
JMM is consultant for OWL, Abbott and Galmed. MN is on the advisory board or a speaker for OWL, Intercept, Echosens and Abbott. He has received research support from Gilead, Galmed, Galectin, Genfit, Conatus, Zydus and Shire, and is a minor shareholder of Anaetos. The other authors have nothing to declare.

Author contribution:
TL, HY, WF, JT, JW, HS, JY, TX, JS – data acquisition, analysis, interpretation. HY also wrote part of the METHODS.
TWHL – data analysis and interpretation, figure preparation and assisted in manuscript writing
ZL, MN, SSM – statistical analysis, edited the paper
AA – provided some of the human liver cancer specimens
ES, JMM – critical reading of the manuscript, intellectual content
SCL - study concept and design, data analysis and interpretation, wrote the manuscript, obtained funding and provided overall study supervision

ABSTRACT

Background & Aims: MAF bZIP transcription factor G (MAFG) is activated by the farnesoid X receptor (FXR) to repress bile acid synthesis. However, expression of MAFG increases during cholestatic liver injury in mice and in cholangiocarcinomas. MAFG interacts directly with methionine adenosyltransferase 1A (MAT1A) and other transcription factors at the E-box element to repress transcription. We studied mechanisms of MAFG upregulation in cholestatic tissues and the pathways by which S-adenosylmethionine (SAMe) and ursodeoxycholic acid (UDCA) prevent the increase in MAFG expression. We also investigated whether obeticholic acid (OCA), an FXR agonist, affects MAFG expression and how it contributes to tumor growth in mice.

Methods: We obtained 7 human cholangiocarcinoma specimens and adjacent non-tumor tissues from patients that underwent surgical resection in California and 113 hepatocellular carcinoma (HCC) specimens and adjacent non-tumor tissues from China, along with clinical data from patients. Tissues were analyzed by immunohistochemistry. MAT1A, MAT2A, c-MYC, and MAFG were overexpressed or knocked down with small interfering RNAs in MzChA-1, KMCH, Hep3B, and HepG2 cells; some cells were incubated with lithocholic acid (LCA, which causes the same changes in gene expression observed during chronic cholestatic liver injury in mice), SAMe, UDCA (100 μM), or FXR agonists. MAFG expression and promoter activity were measured using real-time PCR, immunoblot, and transient transfection. We performed electrophoretic mobility shift, and chromatin immunoprecipitation assays to study proteins that occupy promoter regions. We studied mice with bile-duct ligation, orthotopic cholangiocarcinomas, cholestasis-induced cholangiocarcinoma, diethylnitrosamine-induced liver tumors, and xenograft tumors.

Results: LCA activated expression of *MAFG* in HepG2 and MzChA-1 cells, which required the AP-1, NF-κB, and E-box sites in the *MAFG* promoter. LCA reduced expression of MAT1A but increased expression of MAT2A in cells. Overexpression of MAT2A increased activity of the *MAFG* promoter whereas knockdown of MAT2A reduced it; MAT1A and MAT2A had opposite effects on the AP-1, NF-κB, and E-box–mediated promoter activity. Expression of MAFG and MAT2A increased, and expression of MAT1A decreased, in diethylnitrosamine-induced liver tumors in mice. SAMe and UDCA had shared and distinct mechanisms of preventing LCA-mediated increased expression of MAFG. OCA increased expression of MAFG, MAT2A, and c-MYC but reduced expression of MAT1A. Incubation of human liver and biliary cancer cells lines with OCA promoted their proliferation; in nude mice given OCA, xenograft tumors were larger than in mice given vehicle. Levels of MAFG were increased in human HCC and cholangiocarcinoma tissues compared with non-tumor tissues. High levels of MAFG in HCC samples correlated with hepatitis B, vascular invasion, and shorter survival times of patients.

Conclusions: Expression of MAFG increases in cells and tissues with cholestasis, as well as in human cholangiocarcinoma and HCC specimens; high expression levels correlate with tumor progression and reduced survival time. SAMe and UDCA reduce expression of MAFG in response to cholestasis, by shared and distinct mechanisms. OCA induces MAFG expression, cancer cell proliferation, and growth of xenograft tumors in mice.

Keywords: FXR; obeticholic acid; S-adenosylmethionine; ursodeoxycholic acid

INTRODUCTION

MAFG (V-Maf Avian Musculoaponeurotic Fibrosarcoma Oncogene Homolog G) is a small MAF protein that belongs to the basic leucine zipper family of transcription factors that form heterodimers with nuclear factor-erythroid 2 related factor 2 (NRF2) to bind and activate the antioxidant response element (ARE) present in the promoter region of many genes involved in antioxidant defense[1,2]. MAFG can also homodimerize and act as an ARE repressor[2]. We first reported MAFG's role in liver disease when we found its expression markedly induced during chronic cholestasis[3]. MAFG induction contributed to cholestatic liver injury as it displaced and prevented NRF2 from binding to the ARE, resulting in marked downregulation of the expression of glutathione (GSH) synthetic enzymes and GSH levels[4]. MAFG induction was attenuated during bile duct ligation (BDL) when mice were treated with either S-adenosylmethionine (SAMe) or ursodeoxycholic acid (UDCA) and was completely blocked when these agents were combined[3]. The underlying mechanisms of how SAMe or UDCA inhibit MAFG induction during cholestatic liver injury have not been fully investigated.

We also found that MAFG can directly interact with methionine adenosyltransferase α1 (MATα1), prohibitin 1 (PHB1) and c-MYC at the E-box element (5'-CANNTG-3') and while MATα1 and PHB1 serve as repressors, MAFG and c-MYC are E-box activators[5,6]. MAFG expression increased in both hepatocytes and bile duct epithelial cells during cholestatic liver injury and in murine cholangiocarcinoma (CCA)[5]. Importantly, MAFG expression directly correlated with CCA growth in an orthotopic mouse model[5]. However, the importance of MAFG in human hepatocellular carcinoma (HCC) and CCA has not been investigated.

MAFG was recently identified as a target of farnesoid X receptor (FXR) and serves as a key transcriptional repressor of bile acid synthesis and metabolism[7], providing enterohepatic negative feedback regulation of bile acid synthesis through FXR. Obeticholic acid (OCA) is a potent FXR agonist that was approved in 2016 for the treatment of UDCA unresponsive primary biliary cholangitis (PBC)[8]. This prompted us to question whether OCA treatment may influence MAFG expression and how that relationship impacts the functional behavior of liver cancer cells.

The aims of the current work were to define the underlying molecular mechanisms responsible for MAFG induction during cholestatic liver injury, how therapeutic agents such as SAMe, UDCA and OCA impact these mechanisms, and the clinical significance of MAFG in human liver cancer.

MATERIALS AND METHODS

Materials and reagents

Please see Supplemental Material and Methods for details.

Source of human HCC and CCA with adjacent non-tumorous specimens

Seven human CCA specimens and adjacent benign tissues were obtained from patients that underwent surgical resection at the Cedars-Sinai Medical Center, Los Angeles, CA and 113 HCC specimens and adjacent non-tumorous tissues were obtained from Xiangya Hospital Central South University, Changsha, Hunan province, China. These 113 pairs were fresh-frozen HCC and adjacent benign tissue samples obtained from patients undergoing surgical liver resection from 2013 to 2017 and were kept in liquid nitrogen for storage in the institutional biobank. All human materials were obtained with patients' informed consent. The approval for the use of human samples was obtained from the Institutional Review Board of the Central South University, Xiangya Hospital Authority. The study protocol conformed to the ethical guidelines of the 1975 Declaration of Helsinki as reflected in *a priori* approval by the Institutional Review Boards of Cedars-Sinai Medical Center and the Medical Ethical Committee of Xiangya Hospital Central South University. Both tumor and normal tissue were evaluated histologically to confirm presence or absence of neoplasm.

TCGA dataset from cBioPortal

Graphs showing oncoprint and survival analysis were generated using TCGA dataset from The cBio Cancer Genomics Portal (http://cbioportal.org)[9,10].

Animal experiments

Please see Supplemental Material and Methods for details. Briefly, four different cancer models were included: 1) murine cholestasis-associated CCA model[11], 2) orthotopic CCA model where KMCH cells, in which the expression of MAT1A, c-MYC, or MAFG was consistently varied by overexpression or CRISPR/Cas9 (Clustered Regularly Interspaced Short Palindromic Repeats/CRISPR-associated protein 9), were injected into the left liver lobe of four-week-old male BALB/c nude mice[5], 3) de novo liver carcinogenesis model using deithylnitrosamine (DEN), and 4) xenograft model where six-week-old male BALB/c nude mice were injected subcutaneously with HepG2 ($1x10^6$) or MzChA-1 ($2x10^6$) cells in 100 µl PBS into the right or left flank. From day three after injection mice were divided into three treatment groups (n=8 per group) that received control vehicle (0.9% saline, 100 µl per day by gavage), OCA (30 mg/kg/day in 100 µl saline by gavage), or SAMe (100 mg/kg/day in 100 µl saline by gavage). All procedure protocols, use and the care of the animals were reviewed and approved by the Institutional Animal Care and Use Committee at Cedars-Sinai Medical Center (Los Angeles, CA).

Cell lines and treatments

MzChA-1 (human biliary adenocarcinoma), KMCH (human combined HCC and CCA), Hep3B (human HCC), and HepG2 (human hepatoblastoma) cell lines were cultured in DMEM supplemented with 10% fetal bovine serum (FBS), 100 U/mL penicillin, 0.1 mg/mL streptomycin, and 2 mmol/L L-glutamine. To examine the interplay between MAT2A and MAT1A/c-MYC/MAFG/c-MAF, 6-well plates with $1x10^5$ MzChA-1 or HepG2 cells per well were transfected with vectors overexpressing MATα1, c-MYC, MAFG, or empty vectors (GeneCopoeia, Rockville, MD) for 24 hours using Lipofectamine 2000 according to the manufacturer's protocol. For gene knockdown studies, 10nM siRNA against *MAT1A*, *MAT2A, c-MYC*, or *MAFG* and an equivalent scramble control were delivered into MzChA-1 or HepG2 for 24 hours by Lipofectamine RNAiMAX following

the manufacturer's protocol. Overexpression vectors for MAT1A, MAT2A, c-MYC, and MAFG were previously described[5,12].

MzChA-1, KMCH, Hep3B and HepG2 cells were treated with lithocholic acid (LCA, 0.1-100 µM), SAMe (100 µM), UDCA (100 µM), chenodeoxycholic acid (CDCA, 0.1-100 µM), OCA (0.1-100 µM) or GW4064 (1-50 nM) from one to 16 hours. Effects on gene and protein expression, promoter activity and proliferation were measured as described below. None of the treatments resulted in cell death under these experimental conditions.

Promoter constructs and luciferase assay

Please see Supplemental Material and Methods for details. The human *MAFG* promoter (-1314/+273) was purchased from Genecopoeia (Rockville, MD). Two deletion constructs, -1151/+273 and -422/+273, were created. Site-directed mutagenesis was performed to create mutants for the core motifs of FXR, E-box, NF-κB and AP-1 elements. Constructs containing multimerized enhancer elements, NF-κB (TGGGGACTTTCCGC)X5, AP-1 (TGACTAA)X7 and E-box (CACGTGG)X5 were created.

Histology and immunohistochemistry (IHC)

Formalin-fixed liver and CCA tissues embedded in paraffin were cut and stained with hematoxylin and eosin (H&E) for routine histology. IHC staining of MATα2, MATα1, MAFG, c-MYC, FOSB, JUND, CD31 and IgG was performed with an IHC detection kit from Dako (Carpinteria, CA) or Abcam according to the manufacturer's method. The control with normal mouse IgG showed no staining (not shown).

RNA isolation and gene expression analysis

Please see Supplemental Material and Methods for details.

Chromatin immunoprecipitation (ChIP) and sequential-ChIP (Seq-ChIP) assay

Please see Supplemental Material and Methods for details.

Western blot analysis

Total protein extracts from cells were analyzed using Western blot as described[13]. Please see Supplemental Material and Methods for details.

Electrophorectic mobility shift assay (EMSA)

EMSA was performed as previously described[3]. Please see Supplemental Material and Methods for details.

5-Bromo-2'-deoxyuridine (BrdU) incorporation

BrdU incorporation was measured with a BrdU Detection Kit according to the manufacturer's protocol (BD Biosciences, San Jose, CA). Please see Supplemental Material and Methods for BrdU incorporation after treatment with FXR siRNAs and varying concentrations of OCA.

Apoptosis assay

Please see Supplemental Material and Methods for details.

Statistical analysis

Data are expressed as mean±SEM. Statistical analyses were performed using Student's t-test, ANOVA, and Fisher's test for comparison of two variables, multiple variables, and categorical variables, respectively. For mRNA and protein levels, ratios of

genes and proteins to respective housekeeping densitometric values were compared. MAFG expression (mRNA level) is dichotomized at 2-fold (HCC relative to adjacent non-tumorous tissue) for all clinical variables except for HBsAg status. The MAFG cutoff for HBsAg is set at 2.79-fold with the OptimalCutpoints R package. The optimal cutoff point is determined by minimizing the distance on the receiver operating characteristic (ROC) curve to the left top edge of the diagram, which is equivalent to maximizing the sum of sensitivity and specificity. Nonparametric Mann–Whitney *U* test was used to evaluate the associations between MAFG expression and the binary clinical variables. For survival analysis, log-rank test was used to compare the survival ratio differences between samples with altered MAFG (almost all upregulated) versus normal MAFG expressions. Significance was defined by $p<0.05$.

RESULTS

Mechanisms of MAFG induction by LCA and during cholestasis

We first used an *in vitro* LCA treatment model to dissect the molecular mechanisms of MAFG induction during cholestasis. We have previously established that this in vitro model recapitulates changes in gene expression involving MAFG-interacting proteins observed with chronic cholestatic liver injury models such as BDL and in vivo LCA treatment[14]. The 1.3 kb human *MAFG* promoter contains AP-1, E-box, NF-κB and FXR binding sites (**Supplemental Fig. 1A**). Transfection of HepG2 and MzChA-1 cells with serial deletion constructs revealed that the promoter construct -1151/+273, which contains all four elements, exhibited maximal activity at baseline and in response to LCA treatment for four hours (**Fig. 1A** for MzChA-1 cells and **Supplemental Fig. 1B** for HepG2). Mutation of any of these elements lowered the basal activity (**Fig. 1B**). However, treatment with LCA increased nuclear protein binding only to the E-box, AP-1 and NF-κB sites, while binding to the FXR element fell on EMSA (**Fig. 1C**). Consistently, LCA's inductive effect on the *MAFG* promoter activity was completely lost when the E-box, AP-1 and NF-κB sites were all mutated, but not affected when the FXR binding site was mutated (**Fig. 1D**). In contrast, OCA's inductive effect on the *MAFG* promoter activity was lost when the FXR site was mutated, but not when the E-box, AP-1 and NF-κB sites were mutated (**Fig. 1D**). We therefore focused on the E-box, AP-1 and NF-κB sites in our investigations of the molecular mechanisms responsible for LCA-mediated *MAFG* induction. We used 100 μM LCA treatment for most of our studies because this was the concentration we had used previously that recapitulated the in vivo changes in MAFG expression during cholestatic liver injury[14] that did not cause any overt cell death or apoptosis under our experimental conditions (**Supplemental Fig. 1C**). However, LCA already significantly induced MAFG expression at 0.1 μM in both HepG2 and MzChA-1 cells (**Supplemental Fig. 1D**). CDCA also induced MAFG expression at 1 μM in HepG2 and MzChA-1 cells (**Supplemental Fig. 1E**).

Next, we examined whether LCA treatment altered the expression of transcription factors or proteins that bind to the NF-κB, AP-1 and E-box elements. LCA treatment resulted in a rapid rise in p50, p65, and several AP-1 proteins (c-JUN, JUND, c-FOS and FOSB) at 1-2 hours at the mRNA level (**Fig. 2A & B** for MzChA-1 cells **Supplemental Fig. 2A & B** for HepG2 cells). Although most of the mRNA levels peaked around two hours, the increase in protein levels persisted for 16 hours. For proteins that bind to the E-box, LCA treatment raised c-MYC and MAFG while lowering MAT1A and PHB1 expression at mRNA and protein levels at 2-4 hours (**Fig. 2C, Supplemental Fig. 2C**). In HCC, there is a switch from MAT1A to MAT2A expression that facilitates HCC growth[15,16], but whether MAT2A expression, like HCC, is altered during cholestatic liver injury has not been examined. We found that LCA treatment increased MAT2A mRNA and protein levels at four hours, with levels persisting to 16 hours (**Fig. 2C, Supplemental Fig. 2C**). Changes in MAFG, p50, p65, c-FOS, c-JUN, c-MYC, MAT1A and PHB1 expression during BDL were previously reported[3,14]. Here we show in **Supplemental Figure 3** that induction in FOSB, JUND and MAT2A also occurs during BDL at both mRNA and protein levels.

To define the role of MAT2A in MAFG induction, we examined the effect of varying MAT2A expression on the *MAFG* promoter activity. Overexpression of MAT2A increased *MAFG* promoter activity, whereas knockdown of MAT2A reduced it (**Fig. 3A**). Similar effects were seen at the protein level (**Fig. 3B**). Interestingly, MAT1A and MAT2A exerted opposing effects on AP-1, NF-κB, and E-box-driven promoter activity (**Fig. 3C**).

Regulation of MAT2A expression is regulated by MAT1A/c-MYC/MAFG

We previously reported that *MAT1A* acts as a tumor suppressor while *c-MYC* and

MAFG behave as oncogenes in CCA cells[5]. MAFG and c-MYC are activators of MAT2A, as overexpressing either c-MYC or MAFG raised MAT2A expression, whereas knocking down either one lowered MAT2A expression in the CCA orthotopic model. In contrast, MAT1A represses MAT2A expression (**Supplemental Fig. 4**). We previously showed that c-MYC is a key driver in the murine cholestasis-induced CCA model[11] and consistently, MAT2A expression is much higher in this model (**Supplemental Fig. 5A-C**).

Mechanisms of SAMe and UDCA-mediated inhibition of MAFG expression

We previously reported SAMe and UDCA treatment blocked LCA-mediated induction of MAFG expression[4,14]. The inhibitory effect was enhanced when SAMe and UDCA were used together, suggesting they have different mechanisms. We first examined the effects of SAMe, UDCA or both combined on the *MAFG* promoter activity that is driven by either wild type (WT) or mutant promoter constructs where the NF-κB, AP-1 or E-box was mutated. **Figure 4A** shows that SAMe or UDCA treatment reduced WT *MAFG* promoter activity but this activity was attenuated if any of the three elements were mutated. SAMe or UDCA alone attenuated LCA-mediated induction of both WT and mutant constructs but when they were combined, LCA lost its ability to induce the promoter activity driven by the WT or mutant constructs. These results suggest both SAMe and UDCA target all three elements but by distinct mechanisms that when combined resulted in complete inhibition of the *MAFG* promoter.

To delineate the underlying mechanisms of how SAMe and UDCA exert their inhibitory effects on MAFG expression, we compared treatments with SAMe alone, UDCA alone, together with LCA and without LCA on the expression of the transcription factors that are altered by LCA. SAMe-alone and UDCA-alone treatments reduced LCA-mediated induction of JUND, FOSB, c-JUN and c-FOS (**Fig. 4B**), p65 and p50 (**Fig. 4C**)

comparably. For proteins that bind to the E-box, SAMe induced the expression of MATα1 at baseline and it prevented LCA-mediated fall in MATα1. In contrast, UDCA had no effect on MATα1 expression at baseline or following LCA. SAMe and UDCA raised MNT and PHB1 expression at baseline and both prevented LCA-mediated suppression of MNT and PHB1. Both agents were comparable in attenuating LCA-mediated induction of c-MYC and MATα2 (**Fig. 4D**). We next examined how these treatments affected binding of these proteins to their respective elements using ChIP and Seq-ChIP (for E-box proteins).

SAMe lowered JUND, c-FOS and FOSB binding at baseline whereas UDCA lowered c-JUN and c-FOS binding at baseline. SAMe was more potent in blocking LCA-mediated increase in JUND and FOSB binding, while UDCA was better at blocking the increase in c-JUN binding (**Fig. 5A**). LCA increased p65 and p50 binding to the NF-κB region; SAMe was more effective at reducing p50 binding, but comparable to UDCA at lowering p65 binding after LCA (**Fig. 5B**). At baseline, SAMe raised MATα1 and MNT binding to the E-box region and was more effective than UDCA in lowering c-MYC binding; however, both lowered MATα2 binding comparably (**Fig. 5C**). SAMe was more effective than UDCA at preventing the LCA-mediated fall in MATα1 and MNT and the increase in c-MYC, but they were comparable in lowering MATα2 and raising PHB1 binding following LCA (**Fig. 5C**).

MAFG, MAT1A and MAT2A in DEN-induced HCC in mice

We have shown that MAFG expression is increased in CCA and it enhanced CCA growth and metastasis in an orthotopic model[5]. However, whether MAFG expression is also increased in HCC is unknown. Here we examined the changes in MAFG, MAT1A and MAT2A expression in the DEN model of de novo carcinogenesis. **Supplemental Figure 6** shows MAFG and MAT2A expression is induced in HCC while MAT1A

expression is suppressed at mRNA and protein levels.

Role of MAFG in human liver cancers

Since MAFG positively regulates c-MYC and MAT2A, both of which are induced in human HCC[17], we next examined MAFG expression in 113 HCC patients. Fifty of the 113 patients (44%) had HCC *MAFG* mRNA levels that were at least 2-fold higher than adjacent non-tumorous tissues (**Fig. 6A**). Higher *MAFG* mRNA levels positively correlated with tumor grade (**Fig. 6B**). Higher *MAFG* mRNA levels significantly correlated with a history of hepatitis, alpha-fetoprotein (AFP) levels > 20 IU/mL, and vascular invasion (**Supplemental Figure 7**). Western blotting confirmed higher MAFG and MAT2A protein levels in six pairs of HCC samples as compared to adjacent non-tumorous tissue (**Fig. 6C**) and a positive correlation with vascular invasion (**Fig. 6D, E**). Consistent with our findings, *MAFG* mRNA levels are higher in multiple HCC databases and in the TGCA database, survival of HCC patients with MAFG alterations (mainly amplification and mRNA upregulation) was significantly reduced (**Supplemental Fig. 8A-E**). A similar increase in MAFG expression was observed in human CCA (**Fig. 6F**) and one available database showed MAFG expression is even higher in CCA as compared to HCC (**Supplemental Fig. 9**).

Effect of FXR agonists on MAFG expression and liver cancer phenotype

OCA is a potent FXR agonist[8] that induces *MAFG* promoter activity via the FXR element (**Fig. 1C & D**). This prompted us to examine OCA's effect on the expression of MAFG and related genes. OCA treatment increased *MAFG* mRNA levels in a dose-dependent manner, with significant increase occurring at 0.1 μM in both HepG2 and MzChA-1 cells, although maximum effect was observed at 1 μM (**Supplemental Fig. 10A**). GW4064, another FXR agonist, also induced MAFG expression in a dose-dependent manner, with significant effect observed at 1 nM (**Supplemental Fig. 10B**). OCA

treatment induced MAFG, MAT2A and c-MYC, but lowered MAT1A and PHB1 expression in MzChA-1, HepG2, KMCH, and Hep3B cells at the mRNA and protein levels (**Fig. 7A, Supplemental Fig. 10A, C & D**). GW4064 treatment also led to similar changes at mRNA and protein levels (**Supplemental Fig. 10B, C&D**). Both OCA and GW4064 did not cause any apoptosis at the highest dose under the experimental conditions (**Supplemental Figure 11A**). This translated to increased cell proliferation in all four cell lines (**Fig. 7B, Supplemental Fig. 11B**). Importantly, the effect of OCA required FXR as FXR silencing by FXR siRNA#1 blocked the ability of OCA to induce changes in gene expression and growth (**Fig. 7A & B, see Supplemental Fig. 11C & D** for FXR siRNA knockdown efficiency and effects of FXR siRNA#2 on OCA-mediated changes in gene expression in HepG2 and MzChA-1 cells, and **Supplemental Figure 11E** for OCA-mediated changes in growth in Hep3B and KMCH cells). To see if this was true in vivo, we used the xenograft model and treated mice with either OCA or SAMe as compared to vehicle control starting from three days after injection with HepG2 or MzChA-1 cells. OCA treatment enhanced while SAMe treatment inhibited tumor growth in this model (**Fig. 7C & D**). At the end of the 28 days, OCA treated mice had three to four-fold higher tumor volume as compared to SAMe treated mice (**Fig. 7D)**. Tumors from OCA treated mice have higher MAFG, MATα2, c-MYC but lower MATα1 and PHB1; in contrast, tumors from SAMe treated mice have the exact opposite effects on the same proteins (**Fig. 7E**). Consistent with more rapid tumor growth, OCA treatment increased whereas SAMe lowered vascularization as indicated by CD31 IHC (**Fig. 7F**).

DISCUSSION

Since we first reported hepatic MAFG expression is induced in chronic cholestasis[3] and that this contributes to cholestatic liver injury[4], the physiological role of MAFG has also been shown to provide the enterohepatic negative feedback regulation of bile acid synthesis through FXR[7]. However, in the setting of chronic cholestasis, MAFG induction contributes to the lowering of hepatic GSH synthetic enzymes expression because it can form homodimers as well as heterodimers with c-MAF, a large MAF protein that is also induced in cholestasis[3,4]. These complexes repress ARE-dependent gene expression[2]. Indeed, silencing MAFG protected against the fall in hepatic GSH level and cholestatic liver injury[4]. SAMe and UDCA treatment attenuated the increase in MAFG expression induced by LCA or BDL but they were more effective when combined[4]. This suggested that these agents have distinct mechanisms leading to downregulation of MAFG. One of the major goals of the current work was to elucidate the molecular mechanisms of MAFG induction during cholestasis and how SAMe and UDCA block the induction.

Chronic cholestasis is a major risk factor for development of cholangiocarcinoma[18]. Consistently, we recently showed that sustained MAFG induction potentiated CCA growth in an orthotopic CCA model[5]. However, OCA, the recently approved medication for the treatment of PBC, is a potent FXR ligand[8], but its effect on liver cancer growth has not been examined to the best of our knowledge. In this work we also examined the role of MAFG in the two most common human liver cancers, HCC and CCA, because of the inverse relationship between MAFG and MAT1A, our previous findings that MAT1A is a tumor suppressor for both HCC and CCA[5], and others have shown the ratio of MAT1A to MAT2A expression correlates with HCC survival (the lower the ratio, the lower the survival)[16]. Since MAFG positively regulates MAT2A but negatively regulates

MAT1A, we suspected MAFG might also be dysregulated in HCC. Indeed, our results clearly show MAFG is upregulated in both human HCC and CCA and reveal a previously unknown potential adverse effect of OCA treatment, namely its ability to induce liver cancer growth.

We used the in vitro LCA treatment model to dissect the molecular mechanisms of MAFG induction because this is a model we have validated in the past to recapitulate gene expression changes of those related to MAFG that occur during BDL or LCA in vivo treatment in mice[4,14]. Regarding *MAFG* regulation at the transcriptional level, the human *MAFG* promoter has four key elements - E-box, AP-1, NF-κB and FXR and a mutation of any of these elements lowered the basal promoter activity, suggesting all four are required for basal expression. However, following LCA treatment, nuclear binding to the E-box, AP-1 and NF-κB sites increased but fell for the FXR site. Consistently, mutation of E-box, AP-1 and NF-κB sites individually lowered LCA's inductive effect on the *MAFG* promoter but when all three sites were mutated, LCA lost its ability to induce the *MAFG* promoter. In contrast, mutation of the FXR binding site had no influence on LCA's inductive effect on the *MAFG* promoter. For AP-1 and NF-κB sites, the increased nuclear binding can be explained by an increase in the expression of the transcription factors that bind to those elements. Indeed, the expression of both p65, p50 and many of the AP-1 family members (c-JUN, JUND, c-FOS and FOSB) rapidly increased at both mRNA and protein levels. Our results are consistent with report from Hu et al that LCA can induce the expression of AP-1 and NF-κB family members[19]. For E-box binding proteins, consistent with our previous findings, LCA reduced the expression of MAT1A and PHB1 but increased c-MYC[5,14]. We investigated MAT2A expression here because its expression often correlates inversely with MAT1A and their functions appear to be the opposite of each other at least in HCC, with MAT1A acting as a tumor suppressor whereas MAT2A acting as an oncogene[20]. Indeed, we

found MAT2A expression is rapidly induced following LCA treatment and during BDL, as well as in cholestasis-associated CCA where we reported that MAT1A is down-regulated[5]. MAT2A induction served to enhance MAFG expression and interestingly, we show for the first time that MAT1A and MAT2A exert opposing actions on AP-1, NF-κB and E-box-driven promoter activities, with the former repressing while the latter activating all three. We have shown that MAT2A-encoded protein MATα2 acts as a bona fide transcription factor that binds to and activates the human *BCL2* promoter[12]. We have also shown MATα1's repressive effect on c-MYC expression is independent of DNA methylation or H3K27 trimethylation[5]. The exact mechanisms of how these two highly homologous MAT proteins exert such opposing actions in HCC and CCA cells on gene expression remain to be investigated.

SAMe and UDCA target all the key elements of the human *MAFG* promoter that are induced by LCA. Both agents attenuated the increase in p65 and p50 expression, but SAMe exerted slightly more effect on p50 and UDCA more on p65 in their DNA binding activity. For AP-1 family members, both agents attenuated LCA-mediated increase in their expression with subtle differences. However, SAMe lowered JUND and FOSB binding more than UDCA, which was more effective in lowering c-JUN binding at baseline and after LCA treatment. For E-box binding proteins, the most dramatic difference between SAMe and UDCA is that SAMe increased MATα1 expression and DNA binding whereas UDCA had no effect. SAMe was also more effective than UDCA in reducing c-MYC and increasing MNT DNA binding activity. Both agents exerted comparable effects on MATα2 and PHB1 expression and DNA binding. Combining SAMe with UDCA was more effective than either one alone in preventing LCA-mediated changes in DNA binding activity, suggesting that some of the signaling pathways that these agents triggered are distinct. Our findings are consistent with what has been reported on UDCA's ability to suppress NF-κB and AP-1 DNA binding activities in

multiple different cell types[21-23] and c-MYC expression in colon cancer cells[24]. SAMe has also been shown to inhibit NF-κB activation induced by hepatocarcinogens in rat liver[25] and reduce c-MYC expression by hypermethylating the promoter region of c-MYC[26]. What has not been shown is SAMe's ability to raise MATα1, MNT and PHB1 while lowering MATα2 expression as well as their DNA binding activities to the E-box. The differences between SAMe and UDCA's effects on the expression and binding activity of these proteins could explain why the two agents complement each other's efficacy to prevent LCA-mediated induction of MAFG expression.

We next addressed the question of the significance MAFG in human liver cancers, specifically HCC and CCA. In addition to binding to the ARE, we recently identified that MAFG interacts directly with c-MYC, PHB1, and MATα1 at E-box sequences (5'-CACGTG-3') as a co-activator of E-box-dependent genes that includes c-MYC[5,6]. Consistently, CCA cells overexpressing MAFG resulted in larger tumors with metastasis when tested in an orthotopic model[5]. To examine whether MAFG is indeed important in human liver cancers, we used multiple publically available databases including the TGCA database. MAFG expression is higher in HCC, including hepatitis C virus (HCV)-associated HCCs. Higher MAFG expression in HCC correlated with shorter survival. There is only one publically available CCA database, which compares CCA to HCC, and MAFG expression is even higher in CCA. We verified these findings using our own samples and found that high MAFG expression correlated with tumor grade, vascular invasion, and a history of hepatitis (mainly hepatitis B). Consistent with our finding that MAT2A enhances MAFG expression, a parallel increase in MAT2A expression was seen in the tumors, especially in those with vascular invasion. Interestingly, a previous study showed that HBx protein activated *MAT2A* gene transcription while down-regulating MAT1A expression[27], which could be one of the mechanisms of increased MAT2A expression in HBV-HCCs. Given that MAT2A and MAFG induce each other's

expression and both are activators of the E-box, this is a feed forward mechanism to further enhance growth. This may also explain why 44% of our HCC samples showed high MAFG expression, in contrast to 14% in the TCGA database, as the majority of our HCC samples were due to HBV (at least 70%, status is unknown in 16 patients), whereas only 24% of the HCC patients in the TCGA database had HBV. Besides repressing *MAT1A*, *PHB1* while activating *c-MYC* and *MAT2A*, MAFG is likely to have other targets that can contribute to tumorigenesis. This is a topic of future investigation.

Since persistent MAFG induction led to more aggressive tumors in our orthotopic CCA model[5] and available human cancer databases all support an oncogenic role of this protein, we wanted to examine whether OCA, a potent FXR agonist, would influence MAFG expression and growth behavior in liver and biliary cancer cells. We found OCA increased MAFG, MAT2A, c-MYC but lowered MAT1A and PHB1 expression and this resulted in an increased growth in four different liver and biliary cancer cell lines. The effect required FXR, since FXR silencing prevented OCA-mediated changes in gene expression and growth. This is consistent with our finding that OCA-mediated induction of *MAFG* promoter activity is via the FXR element. The same changes in gene and protein expression observed with OCA also occurred with another FXR agonist, GW4064, at doses as low as 1 nM. Finally, changes in the expression of MAFG, MAT1A, MAT2A, PHB1 and c-MYC as well as growth were confirmed using a xenograft model. While OCA treatment increased MAFG, MAT2A, c-MYC but lowered MAT1A and PHB1 expression, SAMe treatment had the opposite effects. OCA treatment increased growth in the xenograft model using HepG2 and MzCHA-1 cells as well as vascularity, while SAMe treatment had the opposite effects. These findings pose the concern of chronic OCA (and other FXR agonists) administration in patients that already harbor precancerous or cancerous changes in the liver.

In summary, we have clearly demonstrated that MAFG is induced in human HCC and CCA and its up-regulation correlates with worse prognosis in HCC. We provide evidence that LCA induces MAFG expression via activation of AP-1, NF-κB and E-box, all enhancer elements that are present in the human *MAFG* promoter. SAMe and UDCA exert complementary effects to reduce LCA-mediated changes in the expression and DNA binding activity of transcription factors that bind to these elements. We also provide evidence for the first time to our knowledge that OCA treatment of liver and biliary cancer cells caused changes in gene expression that favor increased growth.

REFERENCES

1. Kannan MB, Solovieva V, Blank V. The small MAF transcription factors MAFF, MAFG and MAFK: Current knowledge and perspectives. Biochim Biophys Acta 2012;1823:1841-1846.
2. Lu SC. Glutathione synthesis. BBA-Gen 2013;1830:3143-3153.
3. Yang HP, Ramani K, Xia M, et al. Dysregulation of glutathione synthesis during cholestasis in mice: molecular mechanisms and therapeutic implications. Hepatology 2009;49:1982-1991.
4. Yang HP, Ko K, Xia M, et al. Induction of avian musculoaponeurotic fibrosarcoma proteins by toxic bile acid inhibits expression of GSH synthetic enzymes and contributes to cholestatic liver injury in mice. Hepatology 2010;51:1291-1301.
5. Yang HP, Liu T, Wang J, et al. Deregulated methionine adenosyltransferase α1, c-Myc and Maf proteins interplay promotes cholangiocarcinoma growth in mice and humans. Hepatology 2016;64:439-455.
6. Fan W, Yang H, Liu T, et al. Prohibitin 1 Suppresses Liver Cancers Tumorigenesis in Mice and Humans. Hepatology 2017;65:1249-1266.
7. de Aguiar Vallim TQ, Tarling EJ, Ahn H, et al. MAFG Is a transcriptional repressor of bile acid synthesis and metabolism. Cell Metab 2015;21:298-310.
8. Nevens F, Andreone P, Mazzella G, et al. A Placebo-Controlled Trial of Obeticholic Acid in Primary Biliary Cholangitis. N Engl J Med 2016;375:631-643.
9. Cerami E, Gao J, Dogrusoz U, et al. The cBio cancer genomics portal: an open platform for exploring multidimensional cancer genomics data. Cancer Discov 2012;2:401-404.
10. Gao J, Aksoy BA, Dogrusoz U, et al. Integrative analysis of complex cancer genomics and clinical profiles using the cBioPortal. Science signaling 2013;6:pl1.

11. Yang HP, Li TWH, Peng J, et al. A mouse model of cholestasis-associated cholangiocarcinoma and transcription factors involved in progression. Gastroenterology 2011;141:378-388.
12. Tomasi ML, Ryoo M, Tomasi I,et al. Methionine adenosyltransferase α2 positively regulates B-cell CLL/lymphoma 2 expression in a sumoylation-dependent manner. Oncotarget 2015;6:37706-37723.
13. Yang HP, Cho ME, Li TWH, et al. MiRNAs regulate methionine adenosyltransferase 1A expression in hepatocellular carcinoma. J Clin Invest 2013;123:285-298.
14. Yang HP, Li TWH, Zhou Y, et al. Activation of a novel c-Myc-miR27-Prohibitin 1 circuitry in cholestatic liver injury inhibits GSH synthesis in mice. Antioxidant & Redox Signaling 2015;22:259-274.
15. Cai J, Sun WM, Hwang J,et al. Changes in S-adenosylmethionine synthetase in human liver cancer: molecular characterization and significance. Hepatology 1996;24:1090–1097.
16. Frau M, Tomasi ML, Simile MM, et al. Role of transcriptional and posttranscriptional regulation of methionine adenosyltransferases in liver cancer progression. Hepatology 2012;56:165-175.
17. Ramani K, Mato JM, Lu SC. Role of methionine adenosyltransferase genes in hepatocarcinogenesis. Cancers 2011;3:1480-1497.
18. Blechacz BRA, Gores GJ. Cholangiocarcinoma. Clin Liver Dis 2008;12:131-150.
19. Hu Y, Chau T, Liu HX, et al. Bile acids regulate nuclear receptor (Nur77) expression and intracellular location to control proliferation and apoptosis. Mol Cancer Res 2014;13:281-292.
20. Lu SC, Mato JM. S-adenosylmethionine in liver health, injury and cancer. Physiol Rev 2012;92:1515-1542.

21. Abdel-Latif MM, Inoue H, Reynolds JV. Opposing effects of bile acids deoxycholic acid and ursodeoxycholic acid on signal transduction pathways in oesophageal cancer cells. European J Cancer Prevention 2016;25:368-379.
22. Shah SA, Volkov Y, Arfin Q, et al. Ursodeoxycholic acid inhibits interleukin beta 1 and deoxycholic acid-induced activation of NF-κB and AP-1 in human colon cancer cells. Int J Cancer 2006;118:532-539.
23. Ko WK, Lee SH, Kim SJ, et al. Anti-inflammatory effects of ursodeoxycholic acid by lipopolysaccharide-stimulated inflammatory responses in RAW264.7 macrophages. PLoS One 2017;12:e0180673.
24. Peiró-Jordán R, Krishna-Subramanian S, Hanski ML, et al. The chemopreventive agent ursodeoxycholic acid inhibits proliferation of colon carcinoma cells by suppressing c-Myc expression. Eur J Cancer Prev. 2012;21:413-422.
25. García-Román R, Salazar-González D, Rosas S, et al. The differential NF-kB modulation by S-adenosyl-L-methionine, N-acetylcysteine and quercetin on the promotion stage of chemical hepatocarcinogenesis. Free Radic Res. 2008;42:331-343.
26. Luo J, Li YN, Wang F, et al. S-adenosylmethionine inhibits the growth of cancer cells by reversing the hypomethylation status of c-myc and H-ras in human gastric cancer and colon cancer. Int J Biol Sci. 2010;6:784-795.
27. Liu Q, Chen J, Liu L, et al. The X protein of hepatitis B virus inhibits apoptosis in hepatoma cells through enhancing the methionine adenosyltransferase 2A gene expression and reducing *S*-adenosylmethionine production. J Biol Chem. 2011;286:17168–17180.

FIGURE LEGENDS

Figure 1. **Transcriptional regulation of *MAFG* at baseline and after LCA or OCA treatment**. (**A**) Promoter activity was measured in MzChA-1 cells following transient transfection with serial deletion constructs of the human *MAFG* promoter. Cells were treated during the last four hours of the transfection with vehicle or LCA (100 μM) as described in Methods. Results represent mean ± SEM from four experiments done in triplicates, *p<0.05 vs. empty vector (EV), †p<0.05 vs. control. (**B**) Reporter activities driven by human *MAFG* promoter (1314/+273) that is wild type or mutated in the AP-1, E-box, NF-κB, or FXR elements were compared after transient transfection in MzChA-1 cells. Results represent mean ± SEM from four experiments done in triplicates, *p<0.05 vs. wild type -1151/+273 *MAFG* promoter. (**C**) MzChA-1 cells were treated with LCA for one to 8 hours and processed for EMSA for binding activity to the AP-1, E-box, NF-κB, and FXR elements of the human *MAFG* promoter as described in Methods. OCA treatment served as a positive control for induction of FXR binding. Results represent a total of at least three independent experiments. (**D**) Reporter activities driven by human *MAFG* promoter (1314/+273) that is wild type or mutated in the AP-1, E-box and NF-κB (triple mutation), or FXR element were compared after transient transfection in MzChA-1 cells. Cells were treated with LCA (100 μM), OCA (10 μM) or vehicle controls during the last four hours of the transfection as described in Methods. Results represent mean ± SEM from four experiments done in triplicates, *p<0.05 vs. wild type -1151/+273 *MAFG* promoter + vehicle, †p<0.05 vs 1151/+273 + LCA, ‡p<0.05 vs 1151/+273 + OCA, #p<0.05 vs triple mutant + vehicle, @p<0.05 vs FXR mutant + vehicle.

Figure 2. Effects of LCA treatment on expression of NF-κB, AP-1, and E-box binding proteins. MzChA-1 cells were treated with LCA (100 μM) for one to 16 hours and mRNA and protein levels of NF-κB (**A**), AP-1 (**B**), and E-box (**C**) binding proteins

were measured using real-time PCR and Western blotting as described in Methods. Results are mean ± SEM from three experiments done in triplicates. Numbers below the Western blots are densitometric values expressed as % of 0 hour. *p<0.05 versus 0 hour.

Figure 3. MAT2A positively regulates MAFG expression and exerts opposite effects on AP-1, NF-κB, and E-box-driven promoter activities as compared to MAT1A. MzChA-1 and HepG2 cells were treated with MAT2A siRNA or overexpression vector as described in Methods. (**A**) Shows the effect of varying MAT2A expression on the full-length *MAFG* promoter activity, (**B**) shows the effect on MAFG protein levels in MzChA-1 cells. Results are mean ± SEM from three experiments done in triplicates. Numbers below the Western blots are densitometric values expressed as % of control. *p<0.05 versus control. Scrambled siRNA and empty vector (EV) yielded the same promoter activity and protein levels and were combined as control group. **(C)** MzChA-1 cells were transfected with overexpression vector for MAT1A or MAT2A and effects on AP-1, NF-κB, and E-box-driven promoter activities were measured. Results are mean ± SEM from three experiments done in triplicates, expressed as % of EV control. *p<0.05 versus control.

Figure 4. Effects of SAMe, UDCA and LCA on the human *MAFG* promoter activity and expression of proteins that bind to the AP-1, NF-κB, and E-box. (**A**) MzChA-1 cells were transfected with human *MAFG* promoter (-1314/+273) that is wild type or mutated at the AP-1, NF-κB, or E-box element. During the last four hours of transfection cells were treated with 100 µM of SAMe, UDCA, LCA or vehicle control as described in Methods. Results are mean ± SEM from three experiments done in triplicates, expressed as % of wild type construct. *p<0.05 versus wild type construct, †p<0.05 vs. wild type construct + respective treatment, #p<0.05 vs. wild type construct + LCA

treatment. (**B-D**) MzChA-1 cells were treated with SAMe, UDCA, LCA, alone or together for four hours and protein levels of AP-1 and NF-κB family members and those that bind to the E-box were measured using Western blotting. Numbers below the blots are densitometric values expressed as mean ± SEM % of control. Representative blots are shown from three individual experiments. *p<0.05 vs. control.

Figure 5. Effects of SAMe, UDCA, LCA on occupancy of *MAFG* promoter regions containing AP-1, NF-κB and E-box elements. (**A**) MzChA-1 cells were treated with SAMe, UDCA, LCA, alone or together for 4 hours and were subjected to ChIP analysis for AP-1 family proteins as described in Methods. (**B**) Shows ChIP analysis spanning NF-κB region. (**C**) shows ChIP analysis with MAX followed by Seq-ChIP with MATα1, MATα2, MAFG, c-MYC, MNT, or PHB1 spanning the E-box region. Numbers below the gel images are densitometric values expressed as mean ± SEM % of control. Representative images are shown from three individual experiments. *p<0.05 vs. control.

Figure 6. MAFG and MAT2A expression in HCC and CCA. (**A**) Shows relative *MAFG* mRNA levels from 113 patients with HCC as compared to adjacent liver tissues and (**B**) shows the ratios of *MAFG* mRNA levels in HCC to adjacent non-tumorous tissues separated by HCC grade. (**C**) Shows MAFG and MATα2 protein levels in six pairs of HCC and adjacent tissues on Western blotting. Densitometric values are summarized to the right of the blot. *p<0.05 vs. adjacent tissues. (**D**) shows MAFG and MATα2 protein levels in two representative pairs of HCC and adjacent tissues that have either vascular invasion (VI) or no VI on Western blotting. (**E**) Summarizes protein levels of MAFG and MATα2 from four pairs of HCC patients separated into HCC with VI and HCC without VI. *p<0.05 vs. adjacent tissues, †p<0.05 vs. without VI. (**F**) Shows *MAFG* mRNA levels in

seven CCA samples as compared to adjacent non-tumorous tissues, *p<0.05 vs. adjacent tissues.

Figure 7. Effects of OCA on gene expression and growth in liver cancer cells require FXR. (**A**) HepG2 and MzChA-1 cells ($1x10^5$ cells in 6-well plates) were first transfected with 10 nM FXR siRNA#1 or scramble control for 16 hours by Lipofectamine RNAiMAX following the manufacturer's protocol. This was followed by treatment with OCA (10 µM) for 8 hours and expression of genes was measured using real-time PCR as described in Methods. Results are expressed as mean % of control ± SEM from three experiments done in duplicates, *p<0.05 vs. SC + vehicle, †p<0.05 vs. OCA. (**B**) Following the same treatment protocol with FXR siRNA#1 or scramble control as described above, the effect of OCA (10 µM for 8 hours) on growth in HepG2 and MzChA-1 cells was determined by BrdU incorporation as described in Methods. Results are expressed as mean % of control ± SEM from three experiments done in duplicates, *p<0.05 vs. SC + vehicle, †p<0.05 vs. OCA. (**C**) Effect of OCA on HepG2 and MzChA-1 cell growth in the xenograft model was examined as described in Methods. Representative tumors are shown in the picture. (**D**) HepG2 cells were injected subcutaneously into the right flank in the right figure (*p<0.05, saline vs. SAMe and OCA; n = 8); and MzChA-1 cells were injected subcutaneously into the left flank in the left figure (*p<0.05, saline vs. SAMe and OCA; n = 8), and tumor volumes represented as mean ± SEM were measured over time. (**E**) Protein levels of MATα1, MATα2, c-MYC, MAFG and PHB1 were measured in the tumors at the end of the xenograft experiments (n = 8 each) and normalized to housekeeping control BETA ACTIN. Numbers below the blots represent mean ± SEM densitometric changes expressed as % of vehicle (Veh) control. *p<0.05 vs. vehicle control. (**F**) Vascularization as indicated by CD31 IHC in the tumors at the end of the xenograft experiment. Representative

pictures are shown from n = 8 each. Magnifications are x40 for the images on the left; areas indicated by arrows are further magnified on the right for each group.

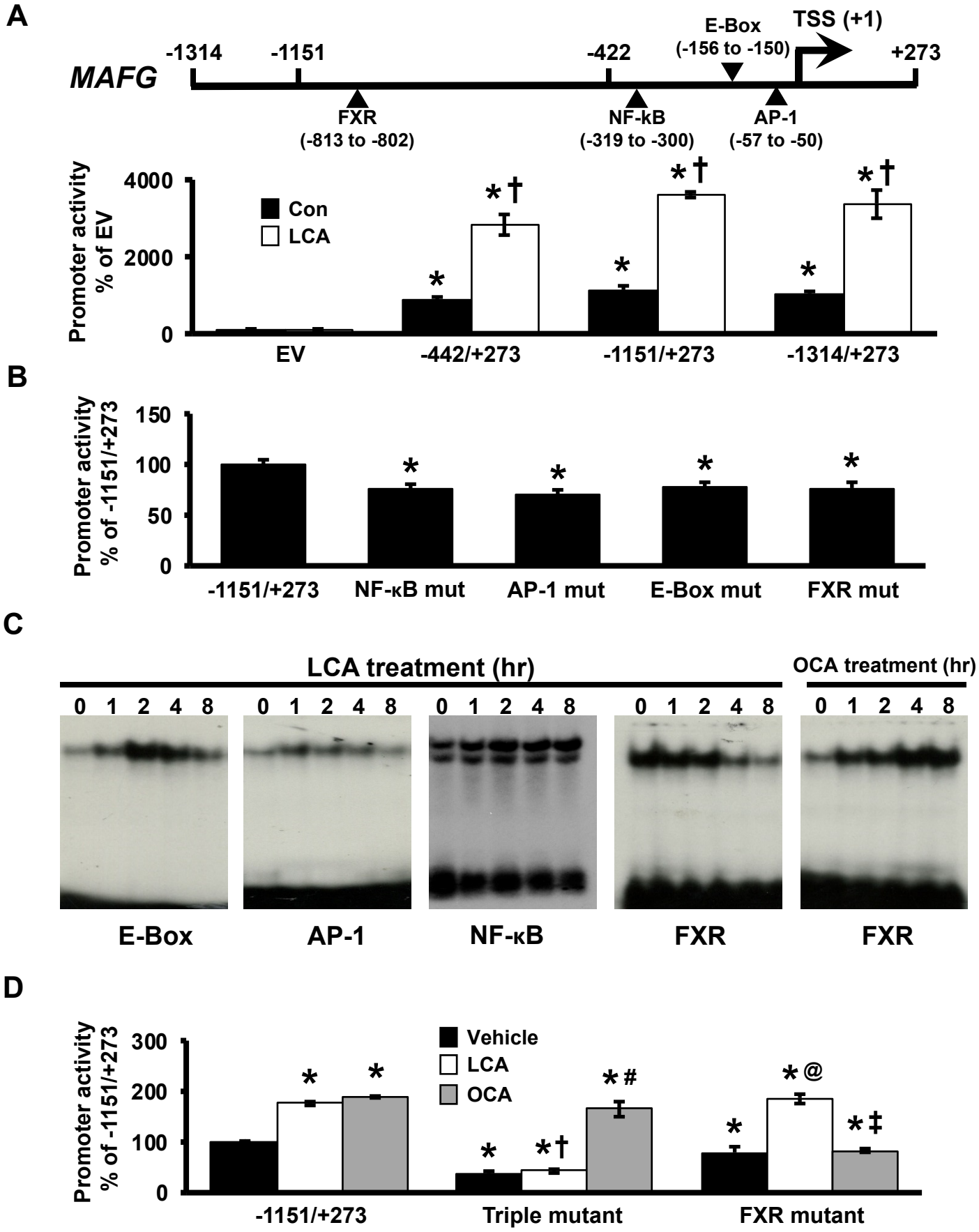
A
MAFG
-1314
-1151
-422
E-Box
(-156 to -150)
TSS (+1)
+273
FXR
(-813 to -802)
NF-kB
(-319 to -300)
AP-1
(-57 to -50)
Promoter activity
% of EV
4000
2000
0
Con
LCA
EV
-442/+273
-1151/+273
-1314/+273
B
Promoter activity
% of -1151/+273
150
100
50
0
-1151/+273
NF-κB mut
AP-1 mut
E-Box mut
FXR mut
C
LCA treatment (hr)
OCA treatment (hr)
0 1 2 4 8
E-Box
AP-1
NF-κB
FXR
FXR
D
Promoter activity
% of -1151/+273
300
200
100
0
Vehicle
LCA
OCA
-1151/+273
Triple mutant
FXR mutant

Figure 1

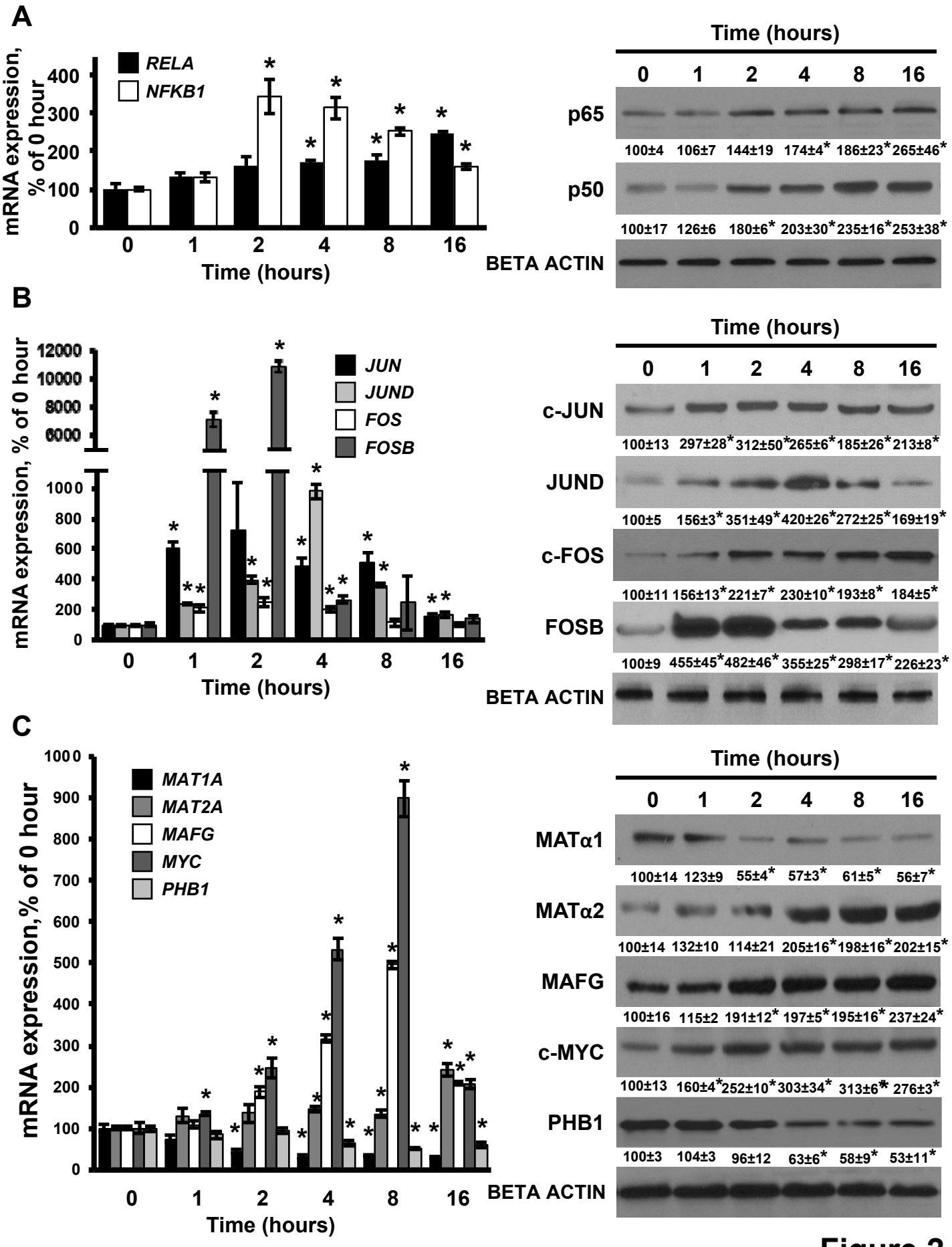
A
mRNA expression, % of 0 hour
RELA
NFKB1
Time (hours)
Time (hours)
0 1 2 4 8 16
p65
100±4 106±7 144±19 174±4* 186±23* 265±46*
p50
100±17 126±6 180±6* 203±30* 235±16* 253±38*
BETA ACTIN
B
mRNA expression, % of 0 hour
JUN
JUND
FOS
FOSB
Time (hours)
Time (hours)
c-JUN
100±13 297±28* 312±50* 265±6* 185±26* 213±8*
JUND
100±5 156±3* 351±49* 420±26* 272±25* 169±19*
c-FOS
100±11 156±13* 221±7* 230±10* 193±8* 184±5*
FOSB
100±9 455±45* 482±46* 355±25* 298±17* 226±23*
BETA ACTIN
C
mRNA expression,% of 0 hour
MAT1A
MAT2A
MAFG
MYC
PHB1
Time (hours)
Time (hours)
MATα1
100±14 123±9 55±4* 57±3* 61±5* 56±7*
MATα2
100±14 132±10 114±21 205±16* 198±16* 202±15*
MAFG
100±16 115±2 191±12* 197±5* 195±16* 237±24*
c-MYC
100±13 160±4* 252±10* 303±34* 313±6* 276±3*
PHB1
100±3 104±3 96±12 63±6* 58±9* 53±11*
BETA ACTIN

Figure 2

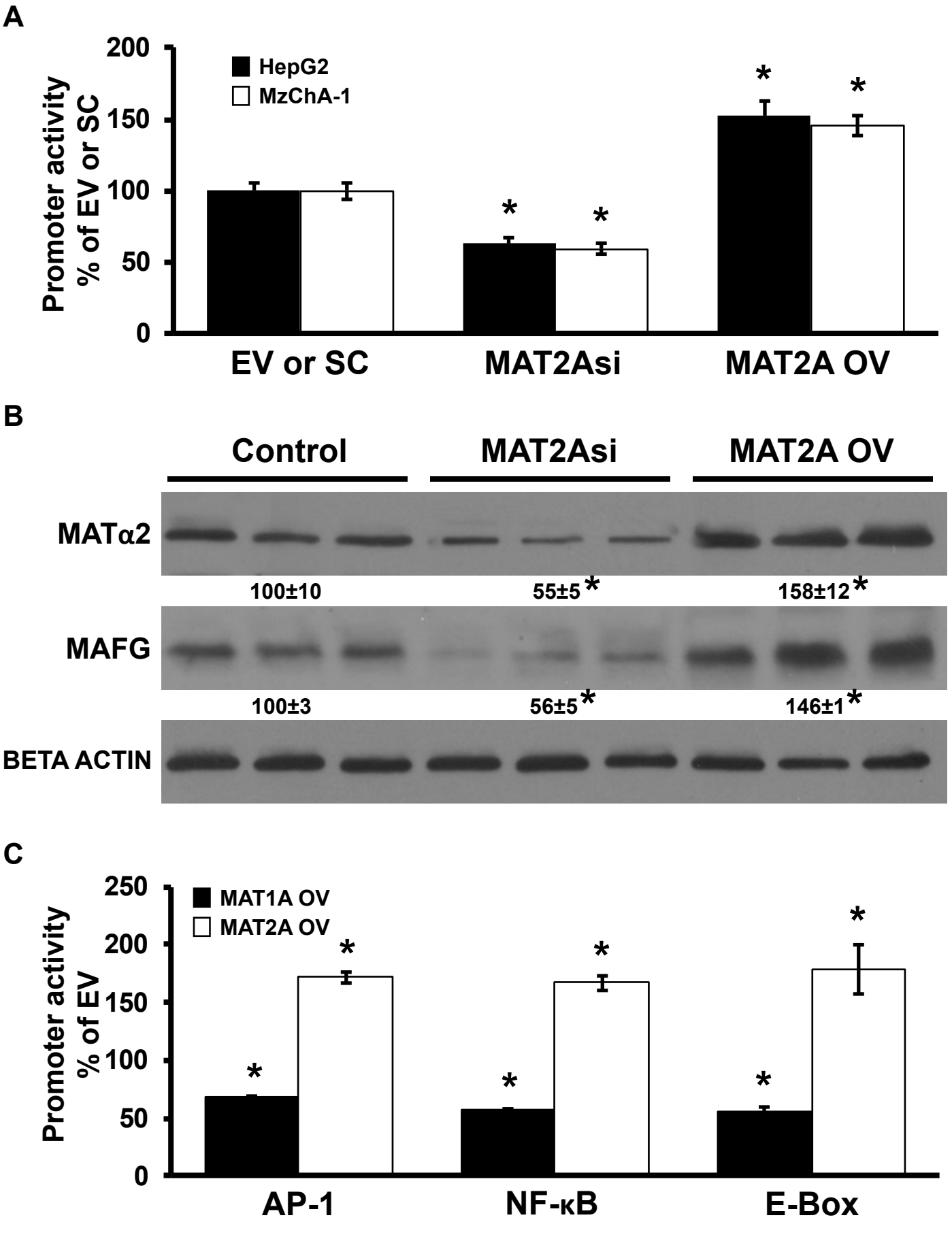
A
Promoter activity
% of EV or SC
200
150
100
50
0
HepG2
MzChA-1
*
*
*
*
EV or SC
MAT2Asi
MAT2A OV
B
Control
MAT2Asi
MAT2A OV
MATα2
100±10
55±5*
158±12*
MAFG
100±3
56±5*
146±1*
BETA ACTIN
C
Promoter activity
% of EV
250
200
150
100
50
0
MAT1A OV
MAT2A OV
*
*
*
*
*
*
AP-1
NF-κB
E-Box

Figure 3

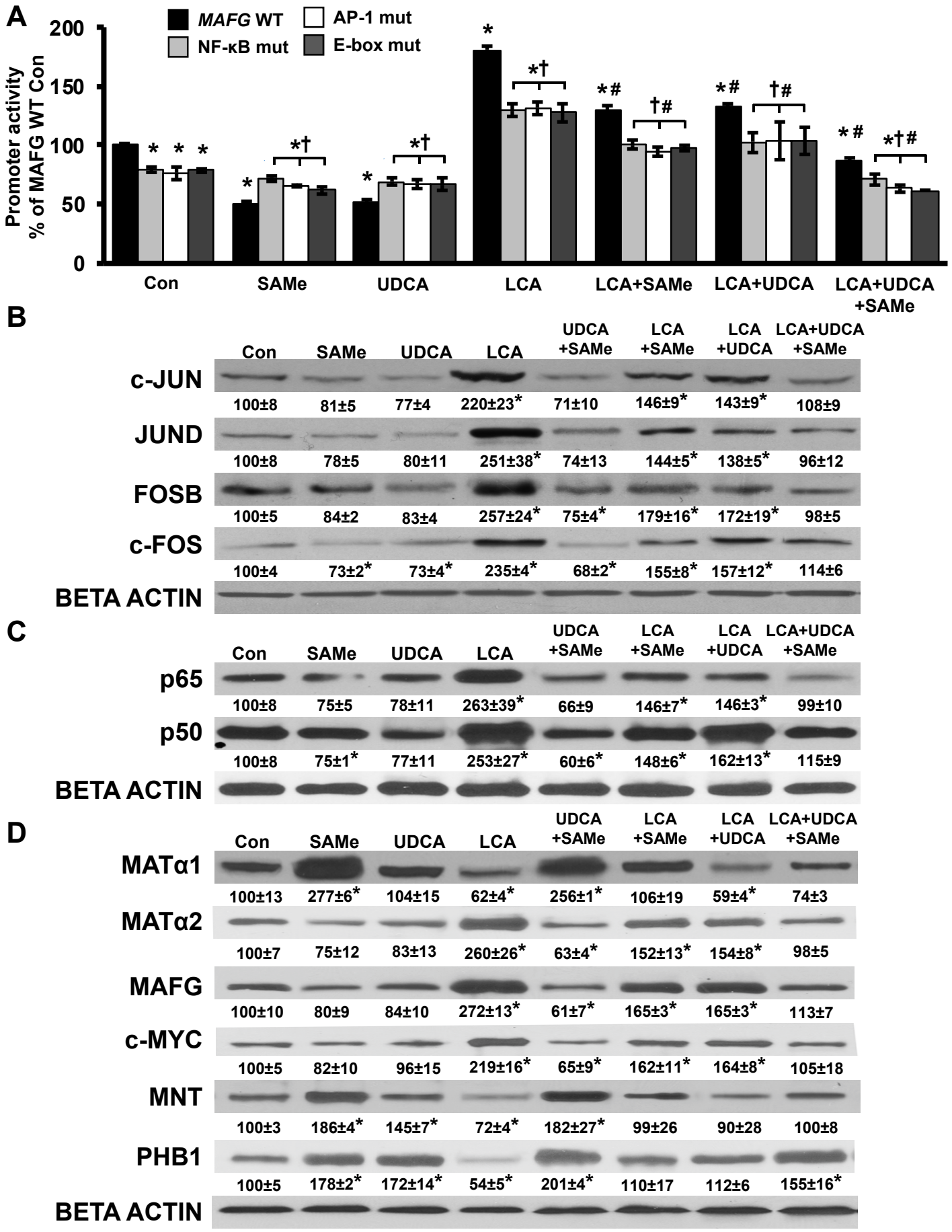
A
MAFG WT
AP-1 mut
NF-κB mut
E-box mut
Promoter activity
% of MAFG WT Con
200
150
100
50
0
Con
SAMe
UDCA
LCA
LCA+SAMe
LCA+UDCA
LCA+UDCA +SAMe
B
Con
SAMe
UDCA
LCA
UDCA +SAMe
LCA +SAMe
LCA +UDCA
LCA+UDCA +SAMe
c-JUN
100±8 81±5 77±4 220±23* 71±10 146±9* 143±9* 108±9
JUND
100±8 78±5 80±11 251±38* 74±13 144±5* 138±5* 96±12
FOSB
100±5 84±2 83±4 257±24* 75±4* 179±16* 172±19* 98±5
c-FOS
100±4 73±2* 73±4* 235±4* 68±2* 155±8* 157±12* 114±6
BETA ACTIN
C
Con
SAMe
UDCA
LCA
UDCA +SAMe
LCA +SAMe
LCA +UDCA
LCA+UDCA +SAMe
p65
100±8 75±5 78±11 263±39* 66±9 146±7* 146±3* 99±10
p50
100±8 75±1* 77±11 253±27* 60±6* 148±6* 162±13* 115±9
BETA ACTIN
D
Con
SAMe
UDCA
LCA
UDCA +SAMe
LCA +SAMe
LCA +UDCA
LCA+UDCA +SAMe
MATα1
100±13 277±6* 104±15 62±4* 256±1* 106±19 59±4* 74±3
MATα2
100±7 75±12 83±13 260±26* 63±4* 152±13* 154±8* 98±5
MAFG
100±10 80±9 84±10 272±13* 61±7* 165±3* 165±3* 113±7
c-MYC
100±5 82±10 96±15 219±16* 65±9* 162±11* 164±8* 105±18
MNT
100±3 186±4* 145±7* 72±4* 182±27* 99±26 90±28 100±8
PHB1
100±5 178±2* 172±14* 54±5* 201±4* 110±17 112±6 155±16*
BETA ACTIN

Figure 4

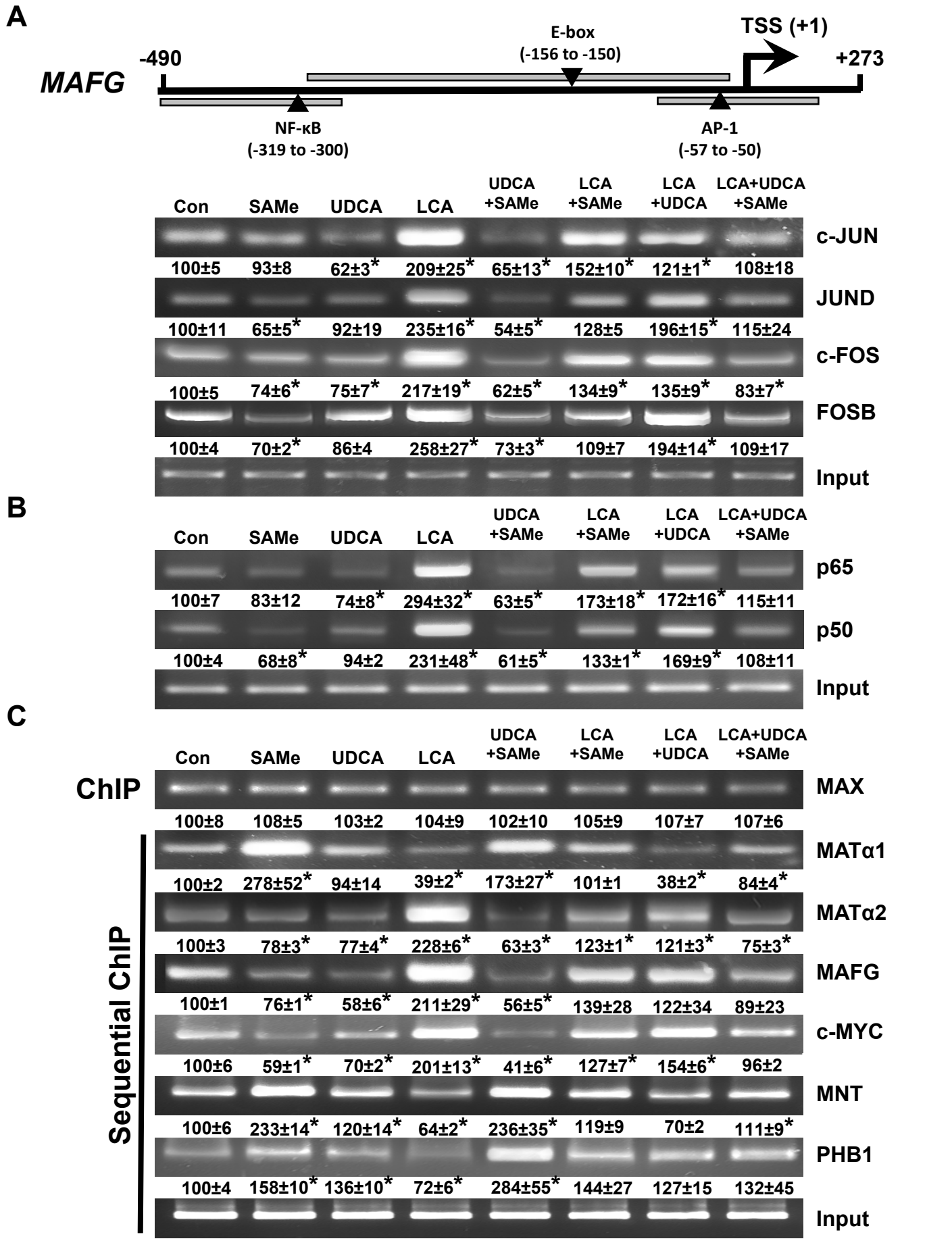
A
MAFG
-490
E-box
(-156 to -150)
TSS (+1)
+273
NF-κB
(-319 to -300)
AP-1
(-57 to -50)
Con
SAMe
UDCA
LCA
UDCA +SAMe
LCA +SAMe
LCA +UDCA
LCA+UDCA +SAMe
c-JUN
100±5 93±8 62±3* 209±25* 65±13* 152±10* 121±1* 108±18
JUND
100±11 65±5* 92±19 235±16* 54±5* 128±5 196±15* 115±24
c-FOS
100±5 74±6* 75±7* 217±19* 62±5* 134±9* 135±9* 83±7*
FOSB
100±4 70±2* 86±4 258±27* 73±3* 109±7 194±14* 109±17
Input
B
p65
100±7 83±12 74±8* 294±32* 63±5* 173±18* 172±16* 115±11
p50
100±4 68±8* 94±2 231±48* 61±5* 133±1* 169±9* 108±11
Input
C
ChIP
MAX
100±8 108±5 103±2 104±9 102±10 105±9 107±7 107±6
Sequential ChIP
MATα1
100±2 278±52* 94±14 39±2* 173±27* 101±1 38±2* 84±4*
MATα2
100±3 78±3* 77±4* 228±6* 63±3* 123±1* 121±3* 75±3*
MAFG
100±1 76±1* 58±6* 211±29* 56±5* 139±28 122±34 89±23
c-MYC
100±6 59±1* 70±2* 201±13* 41±6* 127±7* 154±6* 96±2
MNT
100±6 233±14* 120±14* 64±2* 236±35* 119±9 70±2 111±9*
PHB1
100±4 158±10* 136±10* 72±6* 284±55* 144±27 127±15 132±45
Input

Figure 5

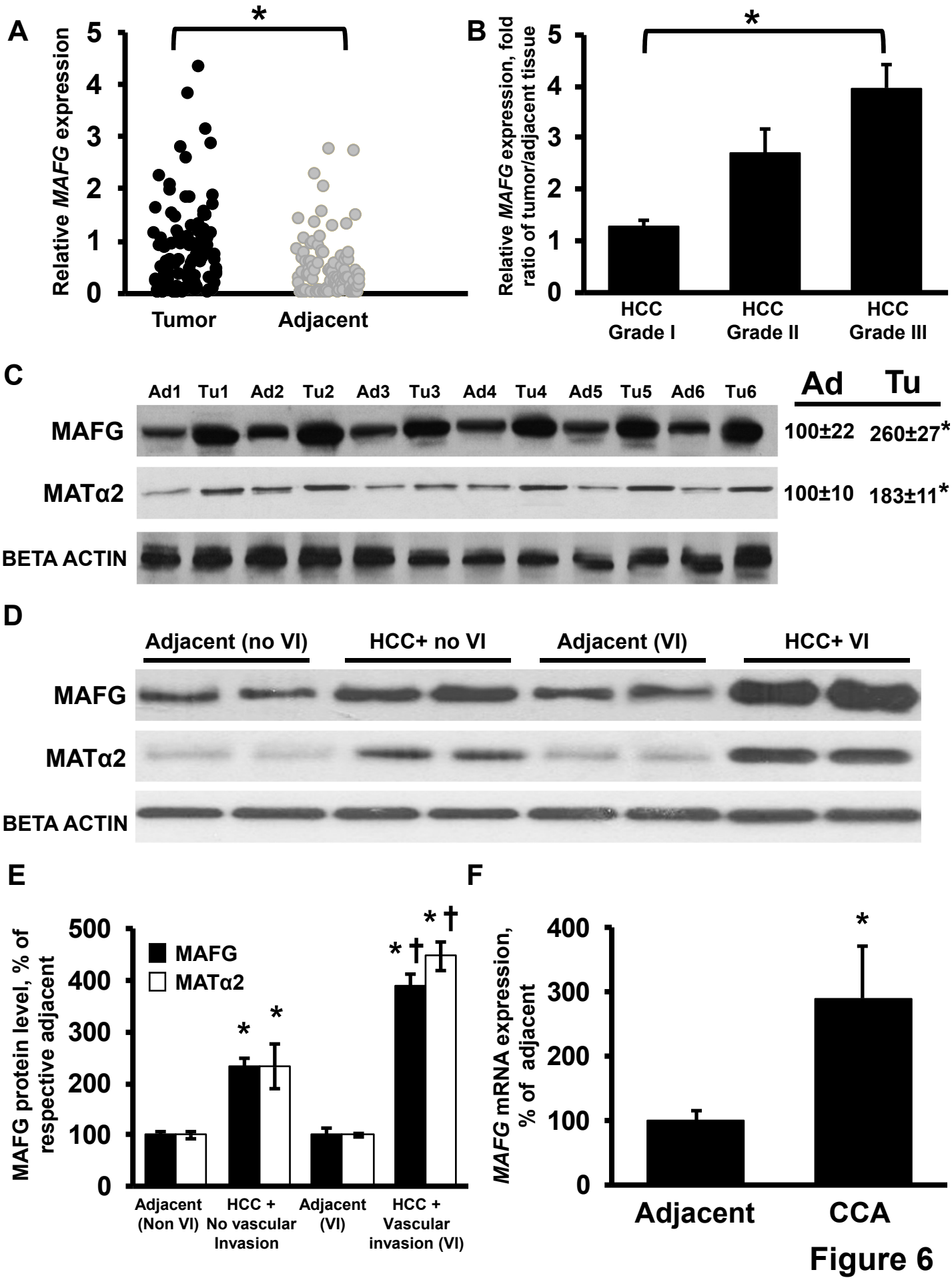
A
Relative MAFG expression
5
4
3
2
1
0
*
Tumor
Adjacent
B
Relative MAFG expression, fold ratio of tumor/adjacent tissue
5
4
3
2
1
0
*
HCC Grade I
HCC Grade II
HCC Grade III
C
Ad1 Tu1 Ad2 Tu2 Ad3 Tu3 Ad4 Tu4 Ad5 Tu5 Ad6 Tu6
Ad Tu
MAFG
100±22 260±27*
MATα2
100±10 183±11*
BETA ACTIN
D
Adjacent (no VI)
HCC+ no VI
Adjacent (VI)
HCC+ VI
MAFG
MATα2
BETA ACTIN
E
MAFG protein level, % of respective adjacent
500
400
300
200
100
0
MAFG
MATα2
*
*
*
*
†
*
*
†
Adjacent (Non VI)
HCC + No vascular Invasion
Adjacent (VI)
HCC + Vascular invasion (VI)
F
MAFG mRNA expression, % of adjacent
400
300
200
100
0
*
Adjacent
CCA

Figure 6

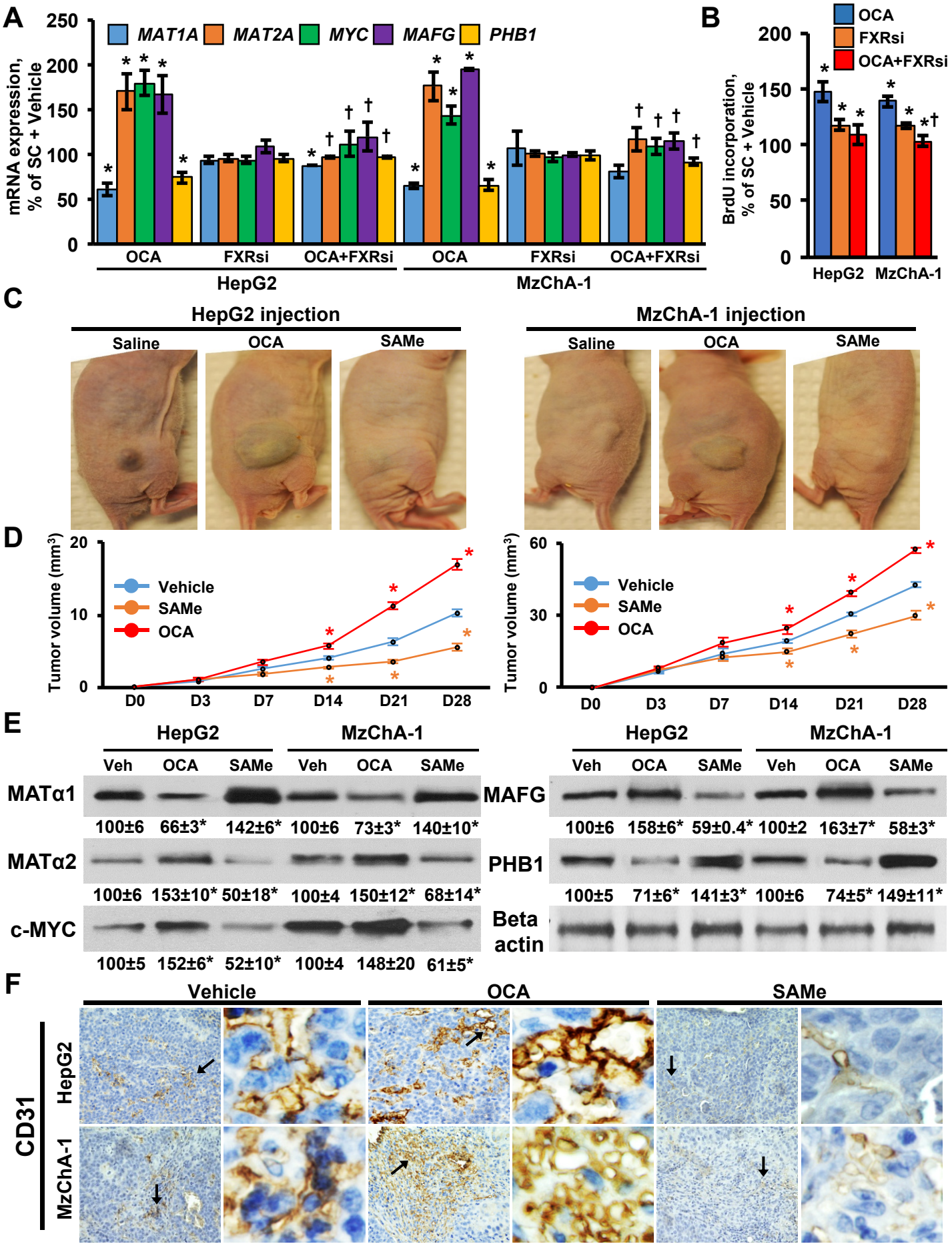
A
mRNA expression, % of SC + Vehicle
MAT1A
MAT2A
MYC
MAFG
PHB1
OCA
FXRsi
OCA+FXRsi
HepG2
MzChA-1
B
BrdU incorporation, % of SC + Vehicle
OCA
FXRsi
OCA+FXRsi
HepG2
MzChA-1
C
HepG2 injection
MzChA-1 injection
Saline
OCA
SAMe
D
Tumor volume (mm3)
Vehicle
SAMe
OCA
D0
D3
D7
D14
D21
D28
E
HepG2
MzChA-1
Veh
OCA
SAMe
MATα1
100±6 66±3* 142±6* 100±6 73±3* 140±10*
MATα2
100±6 153±10* 50±18* 100±4 150±12* 68±14*
c-MYC
100±5 152±6* 52±10* 100±4 148±20 61±5*
MAFG
100±6 158±6* 59±0.4* 100±2 163±7* 58±3*
PHB1
100±5 71±6* 141±3* 100±6 74±5* 149±11*
Beta actin
F
Vehicle
OCA
SAMe
CD31
HepG2
MzChA-1

Figure 7